



Gut Microbiota Mediates the Therapeutic Effect of Monoclonal Anti-TLR4 Antibody on Acetaminophen-Induced Acute Liver Injury in Mice

Xuewei Sun,^{a,b} Qian Cui,^c Juan Ni,^d Xiaoguang Liu,^e Jin Zhu,^a Tingting Zhou,^a HuaYing Huang,^d Ke OuYang,^d Yulong Wu,^b Zhan Yang^a

^aCentre for Diseases Prevention and Control of Eastern Theater, Nanjing, China

^bBinzhou Medical University, Yantai, China

^cAir Force Hospital of Eastern Theater, Nanjing, China

^dThe First Affiliated Hospital of Nanjing Medical University (Jiangsu Province Hospital), Nanjing, China

^eDepartment of Respiratory and Critical Care Medicine, Jinling Hospital, The First School of Clinical Medicine, Southern Medical University, Nanjing, China

Xuewei Sun and Qian Cui contributed equally to this article. Author order was determined by the research group after negotiation.

ABSTRACT Acetaminophen (APAP) overdose is one of the most common causes of acute liver injury (ALI) in Western countries. Many studies show that the gut microbiota plays an important role in liver injury. Currently, the only approved treatment for APAP-induced ALI is *N*-acetylcysteine; therefore, it is essential to develop new therapeutic agents and explore the underlying mechanisms. We developed a novel monoclonal anti-Toll-like receptor 4 (TLR4) antibody (ATAB) and hypothesized that it has therapeutic effects on APAP-induced ALI and that gut microbiota may be involved in the underlying mechanism of ATAB treatment. Male C57BL/6 mice were treated with APAP and ATAB, which produced a therapeutic effect on ALI and altered the gut microbiota and their metabolic pathway, such as *Roseburia*, *Lactobacillus*, *Akkermansia*, and the fatty acid pathway, etc. Furthermore, we verified that purified short-chain fatty acids (SCFAs) could alleviate ALI. Moreover, a separate group of mice that received feces from the ATAB group showed less severe liver injury compared with the mice receiving feces from the APAP group. ATAB therapy also improved the gut barrier functions in mice and reduced the expression of protein zonulin. Our results revealed that gut microbiota plays an important role in the therapeutic effect of ATAB on APAP-induced ALI.

IMPORTANCE In this study, we found the monoclonal anti-Toll-like receptor 4 antibody can alleviate APAP-induced acute liver injury through the change of the gut microbiota, metabolic pathways, and gut barrier function. This work suggested the gut microbiota can be the therapeutic target of the APAP-induced acute liver injury, and we performed the fundamental research for further research.

KEYWORDS gut microbiota, acetaminophen, acute liver injury, TLR4

Acetaminophen (APAP) is one of the most widely used analgesic antipyretics (1), and its overdose is the main cause of acute liver injury (ALI) in Western countries (2, 3). However, effective drugs to treat ALI are lacking and *N*-acetylcysteine (NAC) is the only approved drug for patients who overuse APAP (4, 5), but the application timing is restricted. Therefore, there is an urgent need to develop new drugs and explore their molecular mechanisms.

Pattern recognition receptors are germ line-encoded, evolutionarily conserved receptors that recognize microbe-associated molecular patterns and damage-associated molecular patterns (6). Toll-like receptor 4 (TLR4) is one of the first identified pattern recognition

Editor Jennifer M. Auchtung, University of Nebraska-Lincoln

Copyright © 2022 Sun et al. This is an open-access article distributed under the terms of the [Creative Commons Attribution 4.0 International license](https://creativecommons.org/licenses/by/4.0/).

Address correspondence to Yulong Wu, yulongwu@126.com, or Zhan Yang, breezezhan@126.com.

The authors declare no conflict of interest.

Received 20 February 2022

Accepted 15 April 2022

Published 10 May 2022

receptors and plays an important role in the innate immune response (7). TLR4 also plays an important role in ALI. For example, fetuin-A, a hepatokine, is involved in APAP-induced ALI through the activation of TLR4 (8), and TLR4 antagonism can reduce proinflammatory gene expression (9). Kupffer cells can be activated by TLR4/MyD88 signaling in ALI, TLR4-KO mice were protected from liver necrosis, and similarly, STM28, a TLR4 antagonist, attenuated liver injury and necrosis and reduced creatinine levels (10–12). Evidence shows that agents that can alter the immune response can be developed into therapeutic drugs (13, 14).

TLR4 also plays an important role in gut homeostasis and disease (15); for example, the disruption of TLR signaling increases epithelial proliferation in the transit amplifying zone (16), and the activation of TLR4 in intestinal stem cells reduces proliferation and enhances apoptosis in the small intestine and colon organoids (17, 18). Enhanced epithelial TLR4 signaling is associated with impaired epithelial barrier and microbiota changes (19) and can increase intestinal permeability via an intracellular mechanism involving TLR4-dependent upregulation of CD14 membrane expression and myosin light-chain kinase expression (20, 21). The gut microbiota and gut barrier are also associated with liver disease. In recent years, much attention has been focused on the reciprocal interaction between the gut and liver. This interaction is termed as the gut-liver axis, which refers to the bidirectional relationship between the gut, along with its microbiota, and the liver (22, 23). Several liver diseases are closely related to the gut-liver axis (24–27). For example, *Nlrp6*^{-/-} mice, a model for gut dysbiosis, showed severe liver injury induced by APAP or lipopolysaccharides (LPS) (22), which is associated with early onset of increased intestinal permeability and bacterial translocation (28).

Therefore, we developed a monoclonal anti-TLR4 antibody (ATAB) in our lab that can bind to TLR4 with a high affinity and inhibit LPS-induced TLR4 signaling (29), and we hypothesized that ATAB may have a therapeutic effect on APAP-induced ALI and that the gut microbiota may mediate this effect. Therefore, the present study aimed to determine the therapeutic effects of ATAB on APAP-induced ALI and to examine the role of gut microbiota involved.

RESULTS

APAP-induced ALI was alleviated by ATAB. Mice were treated with APAP (600 mg/kg of body weight) for ALI and then treated with ATAB or with phosphate-buffered saline (PBS) as a control. We found that the ATAB group showed mild liver damage compared with the APAP group. Liver congestion was more serious in the APAP group than in the ATAB group (Fig. 1A). Plasma alanine aminotransferase (ALT) and aspartate aminotransferase (AST) levels were much lower in the ATAB group than in the APAP group (Fig. 1B). In addition, malondialdehyde (MDA) level was lower in the ATAB group than in the APAP group, but superoxide dismutase (SOD), glutathione (GSH), and catalase (CAT) levels were higher in the ATAB group than in the APAP group (Fig. 1C). ALI may induce death in a mouse model, and we found that ATAB improved survival rate (Fig. 1D). After the mice were sacrificed, inflammatory cytokines, lipopolysaccharide (LPS) and chemokines were detected in the plasma and liver tissues, and low expression levels were observed in both of the sample types (Fig. 1E and F). To observe liver injury, hematoxylin and eosin (HE) staining of the liver tissue was performed, which revealed reduced liver cell necrosis in the ATAB group (Fig. 1G).

ATAB altered the gut microbiota composition during ALI treatment. To explore the influence of ATAB, the composition of gut microbiota was evaluated using 16S rRNA gene sequencing. We analyzed the Shannon diversity index and Chao1 index. The ATAB group had higher levels compared with the APAP group (Fig. 2A). The results indicated that the gut microbiota diversity of the APAP-induced ALI mice had changed and that ATAB could enhance the biodiversity of the gut microbiota. We also examined the *Firmicutes/Bacteroidetes* (F/B) ratio and composition of gut microbiota at the phylum level. The results showed that the APAP group had a higher F/B ratio compared with that of the ATAB group. In addition, the composition at the phylum level differed between the two groups. The ATAB group had lower *Firmicutes* and *Bacteroidetes*

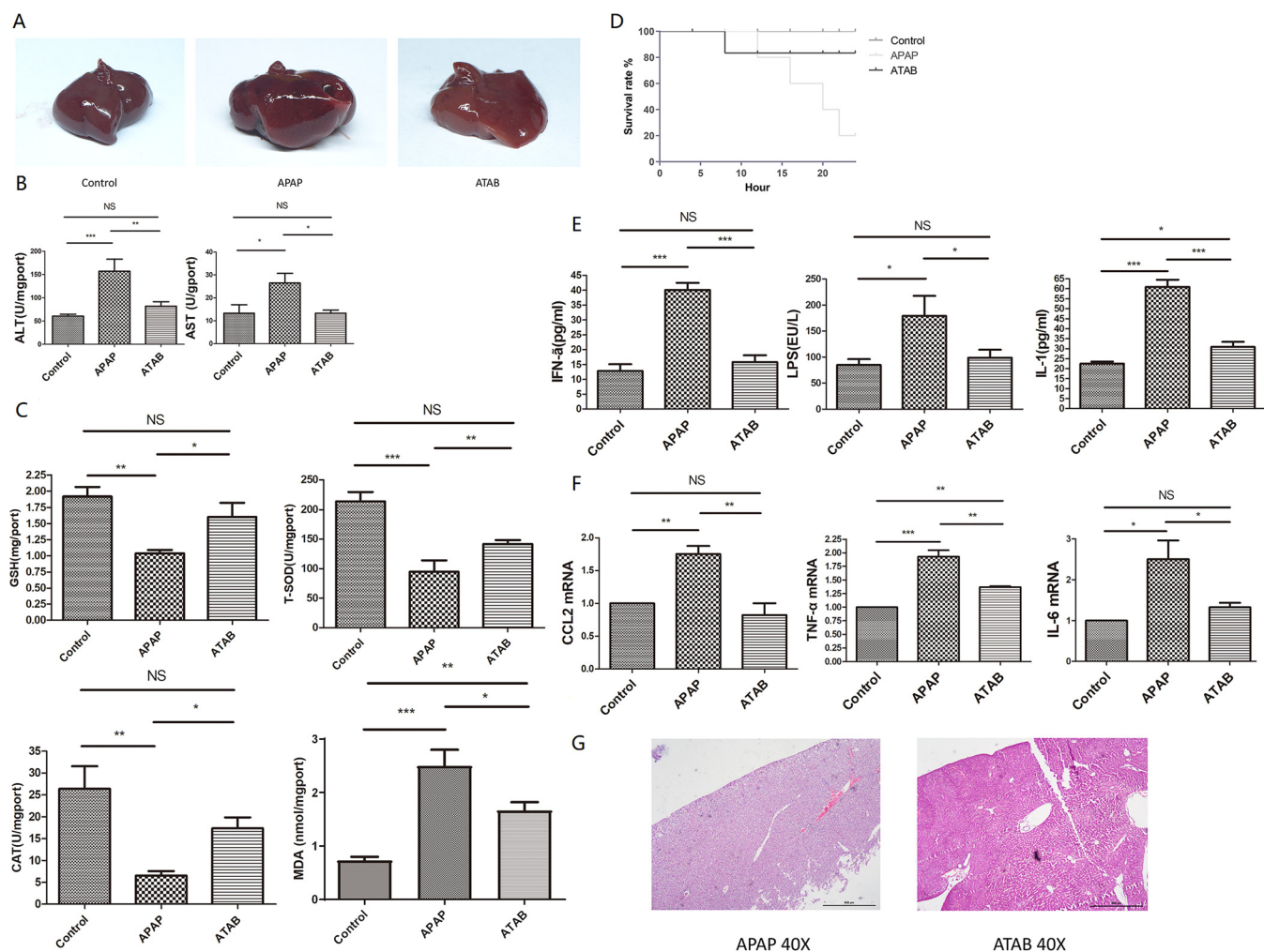


FIG 1 ATAB can alleviate APAP-induced acute liver injury (ALI). (A) Liver congestion is more serious in the APAP group than in the ATAB group. (B) The plasma concentration of ALT and AST is much lower in the ATAB group; $n = 7$ for each group. (C) The ATAB group displayed different liver oxidative stress indices (MDA, SOD, GSH, and CAT) than the APAP group; $n = 8$ for each group. (D) ATAB improved the survival rate for ALI; $n = 8$ for each group. (E and F) The ATAB group exhibited low levels of inflammatory cytokines, LPS, and chemokines in plasma and liver tissues; $n = 7$ for each group. (G) HE staining revealed less necrosis of liver cells in the ATAB group than that in the APAP group. The data are presented as the mean \pm SEM. *, $P < 0.05$; **, $P < 0.01$; and ***, $P < 0.001$ for the comparison.

proportions, but *Proteobacteria* proportions were higher compared with those in the APAP group (Fig. 2B and C). Next, we analyzed the gut microbiota composition using the principal-coordinate analysis (PCoA) and nonmetric multidimensional scaling (NMDS) methods (Fig. 2D and E). The results revealed significant differences among the APAP, ATAB, and control groups, indicating that the use of ATAB can alter gut microbiota composition. The ATAB group had higher abundances of some bacterial genera, such as *Roseburia*, *Lactobacillus*, and *Akkermansia* (Fig. 2F).

ATAB altered the gut microbiota metabolome during ALI treatment. The metabolomic analysis was performed using liquid chromatography-mass spectrometry (LC-MS) to determine whether ATAB can change the gut microbiota metabolome. More than a thousand metabolites were identified, including sugars, amino acids, fatty acids, and organic acids. These compounds are involved in metabolism, genetic information processing, environmental information processing, cellular processes, and organismal systems. The principal-component analysis (PCA) and partial least-squares-discriminant analysis (PLS-DA) methods were used to identify metabolites (we separated the positive and negative charge metabolites), revealing that the APAP group displayed significantly different metabolic profiles compared with the ATAB group (Fig. 3A and B). A heatmap (Fig. 3C) revealed the differences in the metabolites between the two

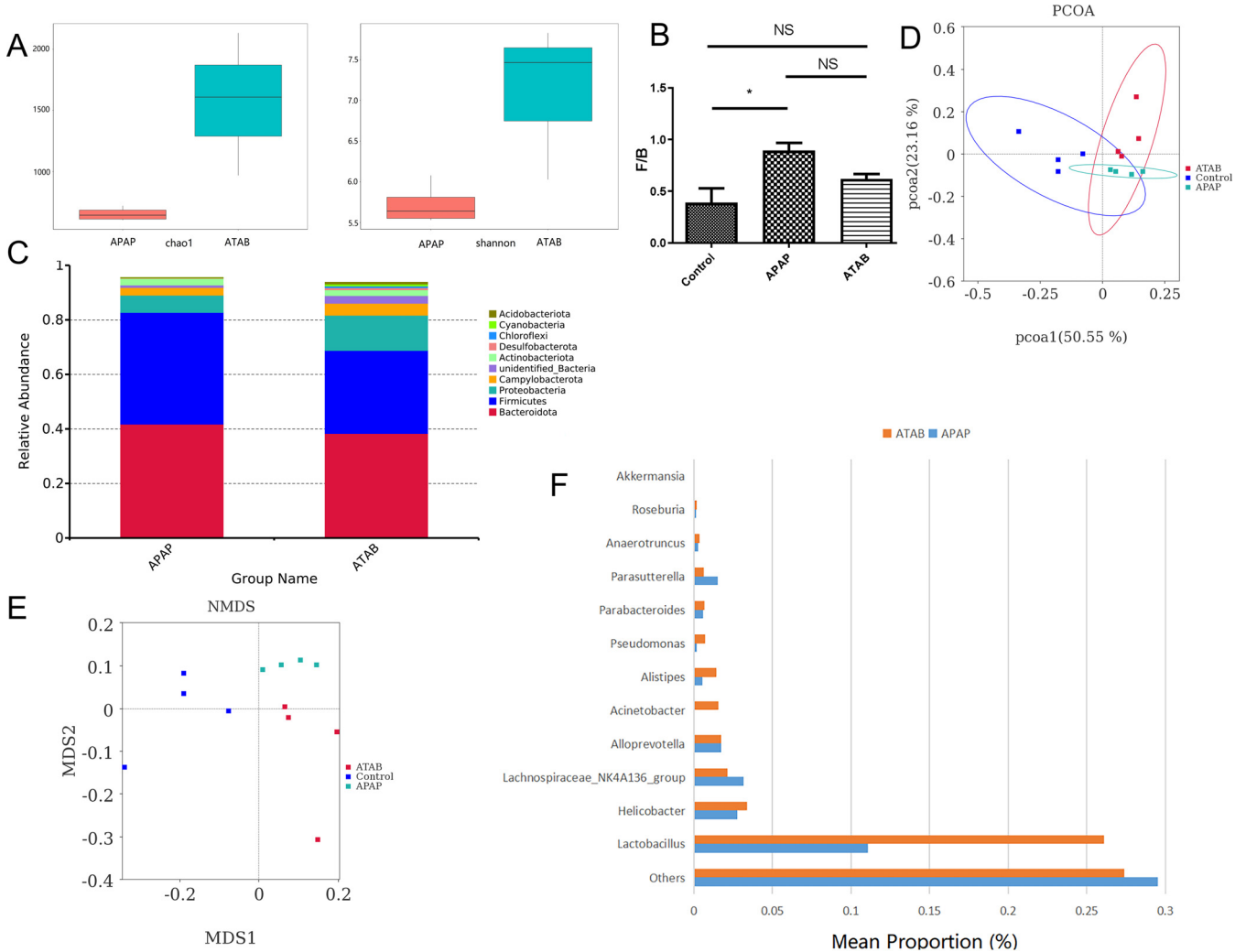


FIG 2 ATAB altered the gut microbiota composition during ALI treatment. (A) The ATAB group had higher Shannon diversity index and Chao1 index. (B and C) The APAP group showed higher F/B ratio of the gut microbiota; the composition at the phylum level differs between the two groups. The ATAB group has lower *Firmicutes* and *Bacteroidetes* levels, but *Proteobacteria* appears to be at a higher level than that of the APAP group. (D and E) The PCoA and NMDS analysis of the gut microbiota. These results show significant difference between APAP, ATAB, and control groups. (F) ATAB had higher abundance of some bacterial genera, such as *Roseburia*, *Lactobacillus*, and *Akkermansia*. $n = 3$ to 4 for each group. The data are presented as the mean \pm SEM. *, $P < 0.05$; **, $P < 0.01$; and ***, $P < 0.001$ for the comparison.

groups. The different metabolites included taurochenodeoxycholic acid, glutaric acid, 2-methylpentanedioic acid, pentadecanoic acid, *N*-acetyl-L-glutamic acid, 3-(4-hydroxy-3-methoxyphenyl) propanoic acid, biotin, and vitamin B₂. We then analyzed the metabolic pathways (Fig. 3D), which showed fatty acid-relevant metabolic pathways, such as fatty acid degradation, linoleic acid metabolism, fatty acid metabolism, fatty acid elongation, and biosynthesis of unsaturated fatty acids. Other noteworthy pathways included retrograde endocannabinoid signaling, biotin metabolism, the PI3K-Akt signaling pathway, and the mTOR signaling pathway.

Based on the 16S rRNA gene sequencing and metabolome analysis, we performed a conjoint analysis, which revealed key bacteria, key metabolites, and their potential correlation; for example, *Lactobacillus*, a key bacterial genus, was correlated with isopropyl myristate, vitamin B₂, and taurocholic acid, etc. (we separated the positive and negative charge metabolites) (Fig. 3E and F). The results provided us with many target bacteria and their metabolites for conducting further research.

Gut microbiota of the ATAB group alleviated ALI via fecal microbiota transplantation. To further analyze the role of gut microbiota in the progression of ATAB treatment, fecal microbiota transplantation (FMT) was performed. The feces of

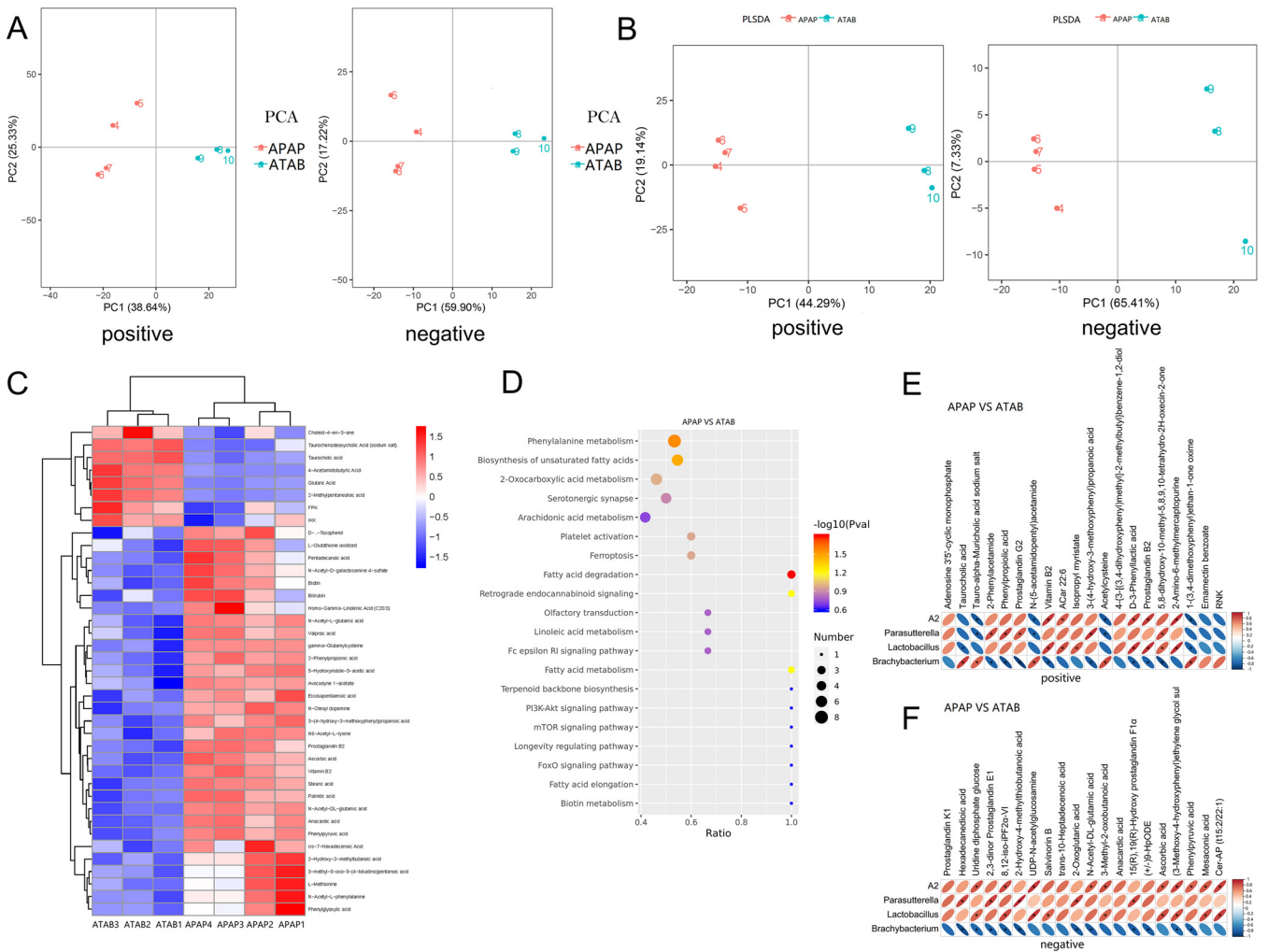


FIG 3 ATAB alters the metabolome of the gut microbiota. (A and B) The PCA and PLS-DA show a significant difference in metabolic profiling in the ATAB and APAP groups (the metabolites were separated for the positive and negative charge). (C) The heatmap shows metabolite differences between the two groups. (D) Various metabolic pathways are shown, including fatty acid degradation, linoleic acid metabolism, fatty acid metabolism, fatty acid elongation, biosynthesis of unsaturated fatty acids, retrograde endocannabinoid signaling, biotin metabolism, PI3K-Akt signaling pathway, and mTOR signaling pathway. (E and F) Conjoint analyses of 16S rRNA gene sequencing and the metabolome show key bacteria and metabolites, as well as the potential correlation (the metabolites were separated for the positive and negative charge); *n* = 3 to 4 for each group.

the ATAB and APAP groups were orally administered to recipients whose gut microbiota had been depleted with broad-spectrum antibiotics (ABX) for 5 days. The gut microbiota of the recipients was similar to that of the donors, indicating that the FMT was successful. After 3 days, the mice were treated with 600 mg/kg APAP and sacrificed 24 h after APAP treatment.

The mice that received feces of the ATAB group had lower interleukin-1 (IL-1), tumor necrosis factor alpha (TNF- α), and IL-6 levels compared with the APAP group (Fig. 4A). HE staining showed that ALI in the recipients of feces of the ATAB group was less severe than that in the recipients of feces of the APAP group (Fig. 4B). However, the amelioration of ALI was not as evident as that observed with direct administration of ATAB. Moreover, the colon tissues of recipients of feces of APAP showed inflammatory cell infiltration (Fig. 4C), indicating that these feces may contribute to inflammation.

ATAB promoted gut barrier function compared with APAP administration. We used fluorescein isothiocyanate (FITC)-dextran oral administration to detect gut barrier function. Approximately 20 h after APAP injection, mice were administered 4 kDa FITC-dextran orally, blood samples were collected after 4 h, and the fluorescence intensity of FITC-dextran in the peripheral blood was measured. The APAP group showed high fluorescence intensity, whereas the ATAB group showed lower fluorescence intensity in

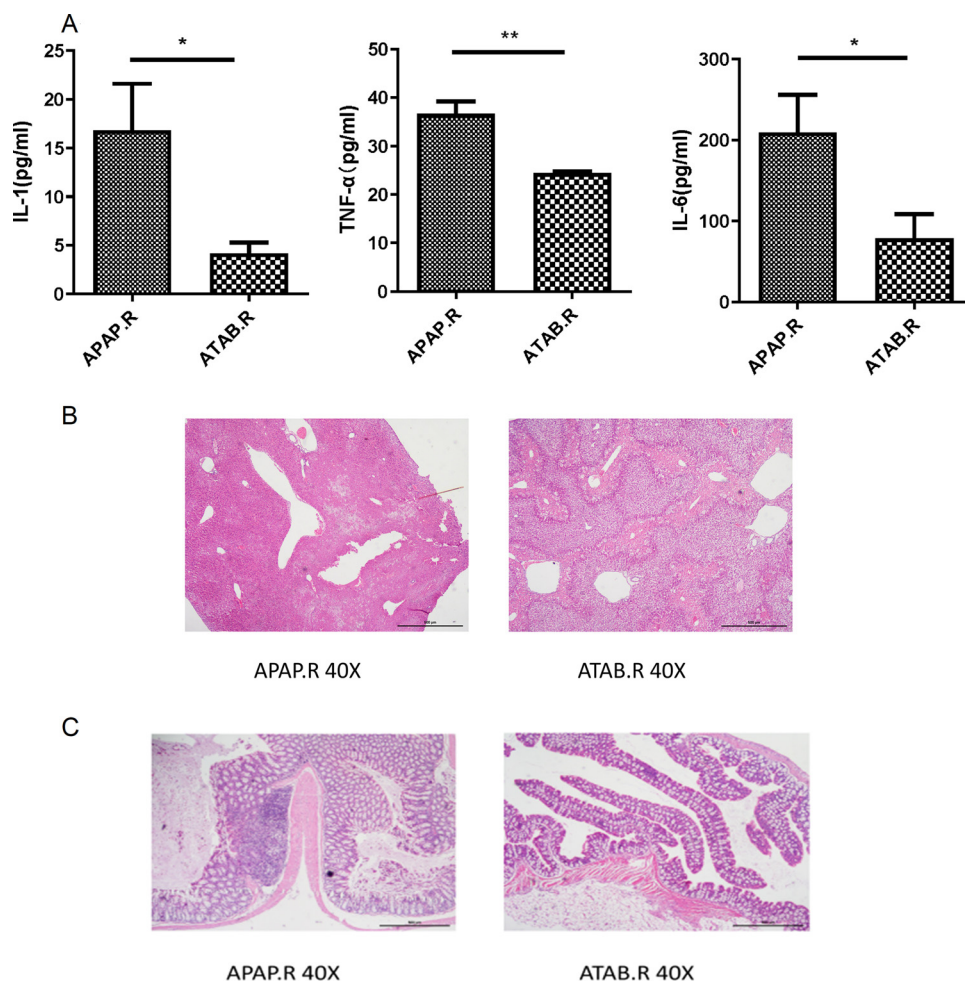


FIG 4 Gut microbiota from the ATAB group can alleviate ALI through the FMT. (A) The mice that received ATAB feces had lower IL-1, TNF- α , and IL-6 levels than the mice in the APAP group. (B) HE staining shows that ALI in the mice receiving feces of the ATAB group was less severe than that observed in mice receiving feces of the APAP group. (C) The colon tissues of mice receiving feces of the APAP group display inflammatory cell infiltration, but the mice receiving feces of the ATAB group show no obvious change; $n = 4$ to 5 for each group. The data are presented as the mean \pm SEM. *, $P < 0.05$; **, $P < 0.01$; and ***, $P < 0.001$ for the comparison.

the serum (Fig. 5A). We also observed colon tissues, and the APAP group showed extravasation of FITC-dextran, whereas the ATAB group showed the confinement of FITC-dextran to the colon lumen (Fig. 5B). As zonulin is a modulator of the intestinal epithelial cell tight junctions, we quantified the protein content in the colon tissue of mice from APAP and ATAB groups using the enzyme-linked immunosorbent assay (ELISA) method. The results revealed that the APAP group had higher zonulin levels than the ATAB group (Fig. 5C). Therefore, our results demonstrated that ATAB can promote gut barrier function.

Short-chain fatty acids can alleviate APAP-induced ALI without ATAB. Metabolomic analysis revealed that the fatty acid metabolic pathway differed between the two groups, so the well-established metabolites, short-chain fatty acids (SCFAs), were chosen to determine whether they might influence APAP-induced ALI. The SCFAs were dissolved in water and were given to mice for free drinking for 7 days. Thereafter, APAP was injected, and the blood and liver tissues of mice were collected after 24 h. The results showed that liver congestion was milder (Fig. 6A), and plasma ALT and AST levels were much lower in the SCFAs group (Fig. 6B) than in the control group. HE staining showed reduced liver cell necrosis in the SCFAs group (Fig. 6C). In addition, the survival rate was 100% in the SCFAs group but only 40% in the APAP group (Fig. 6D). The

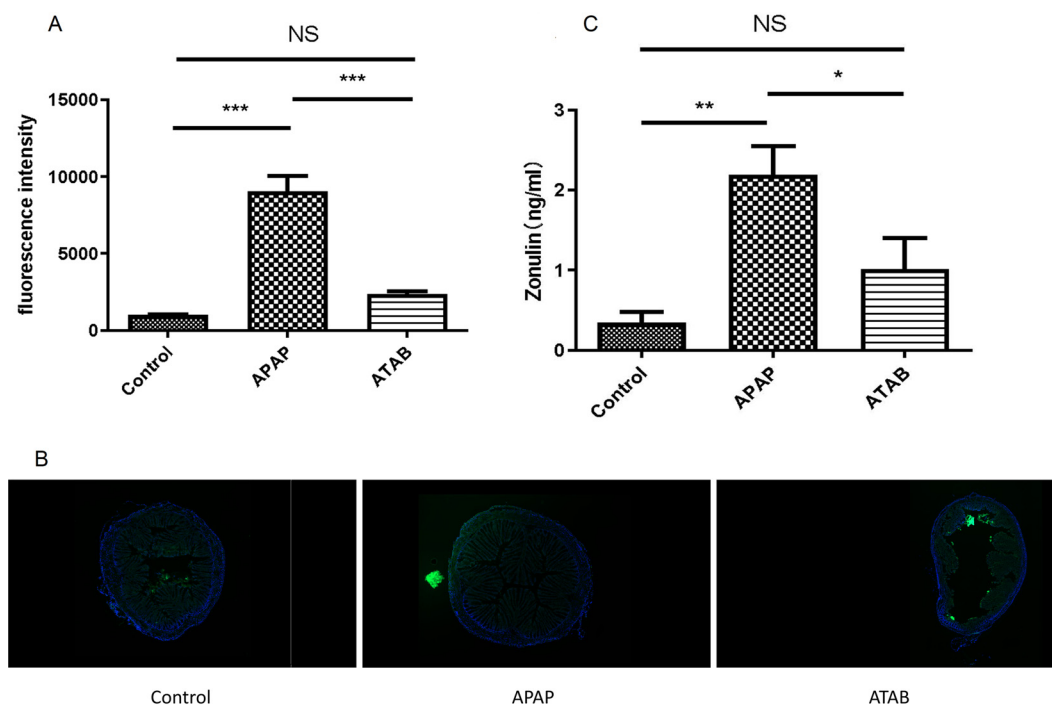


FIG 5 ATAB can promote gut barrier functions. (A) The APAP group shows greater fluorescence intensity in the serum than the ATAB group. (B) In the colon tissues, the APAP group displays FITC-dextran extravasation, while FITC-dextran in the ATAB group was mainly confined to the colon lumen. (C) The ATAP group displayed greater levels of the protein zonulin compared with the ATAB group; $n = 3$ for each group. The data are presented as the mean \pm SEM. *, $P < 0.05$; **, $P < 0.01$; and ***, $P < 0.001$ for the comparison.

treatment effect of SCFAs was evident, as they alleviated APAP-induced ALI without ATAB administration.

DISCUSSION

In this study, we investigated the therapeutic effect of ATAB on APAP-induced ALI and analyzed the role of the gut microbiota, gut metabolism, and gut barrier in this process.

We found that ATAB treatment altered the composition of gut microbiota, including the F/B ratio and the composition at the phylum level. We observed that specific bacteria differed between the ATAB and APAP groups, such as *Lactobacillus*, *Akkermansia*, and *Roseburia*. *Lactobacillus* is a well-studied probiotic, and some specific strains are useful in treating liver disease; for example, *Lactobacillus rhamnosus* LGG can ameliorate liver injury and hypoxic hepatitis in a rat model of cecal ligation and puncture (CLP)-induced sepsis (30), *Lactobacillus plantarum* CMU995 can ameliorate alcohol-induced liver injury by improving both the intestinal barrier and antioxidant activity (31), and *Lactobacillus acidophilus* LA14 can alleviate liver injury induced by D-GalN in rats (32). ATAB may enhance the abundance of *Lactobacillus* in the gut microbiota and play a role in the alleviation of ALI. *Akkermansia muciniphila*, a novel probiotic, has recently attracted increasing attention. A recent study showed that *Akkermansia muciniphila* can protect mice from HFD/CCl4-induced liver injury (33). In our study, ATAB enhanced *Akkermansia* levels, which may contribute to the therapeutic effect. *Roseburia* is another bacterial genus that is more abundant in the ATAB group. *Roseburia* can ameliorate alcoholic fatty liver in mice (34) and is the source of propionate and butyrate in the gut (35–37). Therefore, these bacteria may have different probiotic functions.

FMT research is necessary for microbiome studies to transform correlation to causation (38); therefore, we performed FMT to evaluate the exact function of the gut

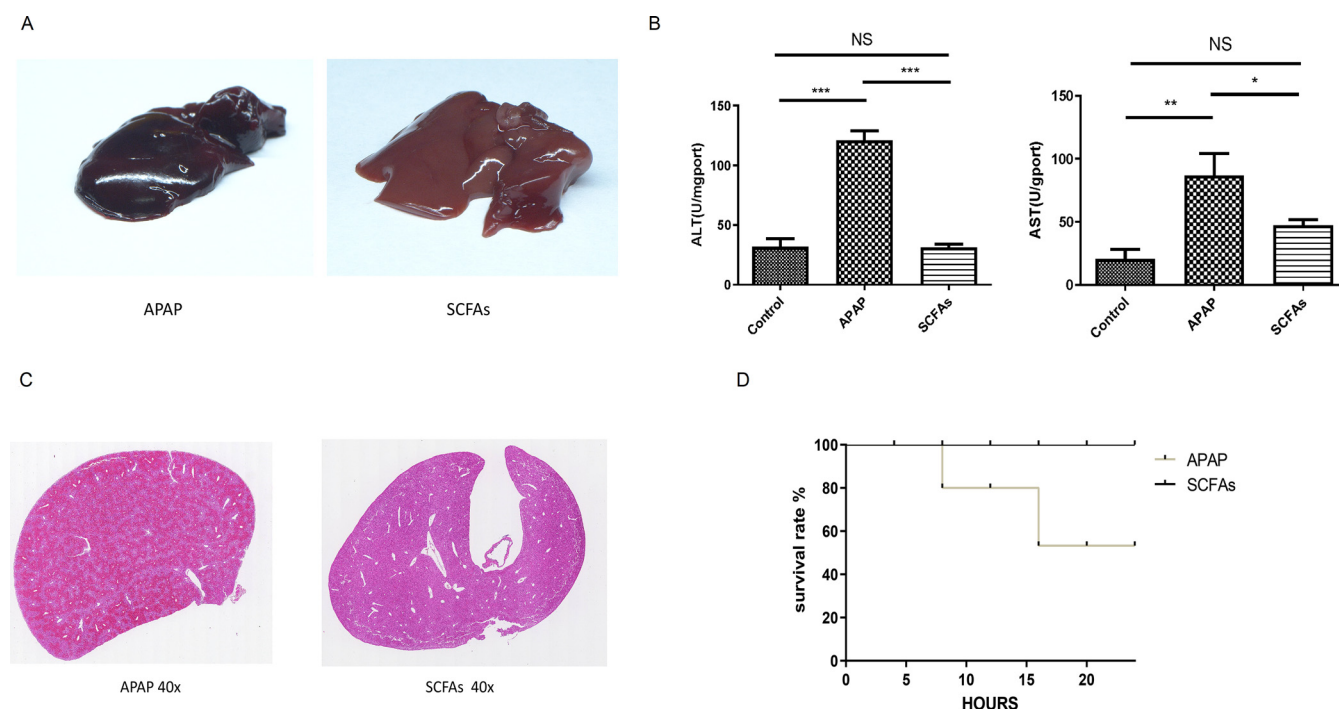


FIG 6 Short-chain fatty acids (SCFAs) can alleviate APAP-induced ALI without ATAB. (A) Liver congestion was milder in the SCFAs group. (B) Plasma ALT and AST levels were lower in the SCFAs group. (C) HE staining shows decreased liver cell necrosis in the SCFAs group. (D) The survival rate was 100% in the SCFAs group compared with 40% in the APAP group; $n = 5$ to 7 for each group. The data are presented as the mean \pm SEM. *, $P < 0.05$; **, $P < 0.01$; and ***, $P < 0.001$ for the comparison.

microbiota. Feces from the ATAB group can alleviate ALI, although the therapeutic effect is not as obvious as that of ATAB, suggesting that the gut microbiota and metabolites mediate the therapeutic effect of ATAB, at least in part. Thus, ATAB may also function via other underlying mechanisms that treat APAP-induced ALI.

The importance of metabolites in gut microbiota studies is acknowledged, as they exert their effects as signaling molecules and substrates for metabolic reactions (39). In this study, we found several metabolic pathways that differ between the ATAB and APAP groups, such as the fatty acid and bile acids relevant metabolic pathway. The synthesis and secretion of bile acids is one of the most important functions of the liver, and it influences the gut-liver axis. Lipopolysaccharides from the gut bacteria can enter the liver through portal circulation, which can combine with TLR4 and aggravate the inflammatory response causing liver cell death (40). Therefore, this may also represent the mechanism by which ATAB alleviates liver injury.

SCFAs are the products of bacteria in the cecum and colon (41), have many beneficial effects (37), and are also involved in fatty acid metabolism. However, there have been few studies on SCFAs and liver injury. We directly provided SCFAs to APAP-treated mice and found that SCFAs alleviated ALI unexpectedly. Metabolites of the gut microbiota influence physical health; therefore, we performed metabolomic analysis to reveal multiple metabolites to be further explored as research targets.

Intestinal barrier function is associated with intestinal and extraintestinal diseases, including liver disease (27, 42). APAP increases intestinal permeability, which may explain the induction of ALI but not the direct cytotoxicity to liver cells (43, 44). We found that ATAB could improve gut barrier functionality, and this may contribute to the mechanisms underlying the therapeutic effects of ATAB in ALI.

To the best of our knowledge, this is the first study to explain the role of the gut microbiota during ATAB therapy for APAP-induced ALI. However, this study has certain limitations. First, the causal relationship between the gut microbiota and the therapeutic effect of ATAB was analyzed insufficiently; for example, we did not perform research into specific bacterial strains. Different bacterial strains between the two groups should

TABLE 1 Real-time PCR primer pairs

Primer pair	Sequence (5' to 3')
IL-6	
Forward	TGATGCACTTGCAGAAAACA
Reverse	ACCAGAGGAAATTTTCAATAGGC
CCL2	
Forward	CCTGCTGTTACAGTTGCC
Reverse	ATTGGGATCATCTTGCTGGT
TNF- α	
Forward	ACGTCGTAGCAAACCACCAA
Reverse	TAGCAAATCGGCTGACGGTG

be screened and their function verified in APAP-induced ALI. For instance, previous research has shown that *Lactobacillus acidophilus* LA14 could alleviate liver injury (32). Regarding the metabolites, we verified the function of SCFAs in ALI; however, we only observed that they can alleviate ALI, but the exact mechanism is still unclear and requires further research. Second, ATAB can improve gut barrier function; however, the molecular mechanism is unknown. Gut barrier function requires further analysis because of its importance in liver disease.

In conclusion, we reported a new therapeutic method for APAP-induced ALI in a mouse model and analyzed the role of gut microbiota in this therapy. The fundamental data provided in this study may provide the foundation for further studies in this research area, leading to the development of new therapeutic strategies to treat APAP-induced ALI.

MATERIALS AND METHODS

Mouse model and treatment. Male C57BL/6 mice (age, 4 to 6 weeks) were obtained from the biotechnology limited company of Sibeifu (Beijing, China). The mice were housed in a specific pathogen-free animal experiment facility at $23 \pm 1^\circ\text{C}$ and $53\% \pm 2\%$ humidity with a 12-h light/dark cycle. The mice were fed a standard laboratory diet (*ad libitum*) in individual standard stainless steel cages. To eliminate sex as an influencing factor in our experiments, we used only male C57BL/6 mice in this study. Therefore, it is important to bear in mind that the results for female mice may be different. All animals were fed adaptively for 1 week before the experiment. The mice were randomly assigned into three groups (APAP group, ATAB group, and control group; $n = 8$ in each group). Members of the APAP group were intraperitoneally injected with 600 mg/kg acetaminophen dissolved in PBS. The ATAB group was orally gavaged with 5 mg/kg ATAB 2 h after acetaminophen injection, and the control group was intraperitoneally injected with the same volume of PBS. For antibiotics treatment, mice received vancomycin (100 mg/kg), neomycin sulfate (200 mg/kg), metronidazole (200 mg/kg), and ampicillin (200 mg/kg) intragastrically once daily for 5 days. Mice were not fasted before APAP treatment and were sacrificed at 24 h after APAP treatment.

The mouse experiments were carried out in accordance with the recommendations of the ethics provision for experiments on mice of the ethics committee of the Centre for Diseases Prevention and Control of Eastern Theater. The protocol was approved by the ethics committee of the Centre for Diseases Prevention and Control of Eastern Theater.

Determination of biochemical parameters of serum and tissues. The serum ALT and AST levels were detected by detection kit (Jiancheng Bioengineering, Nanjing, China). T-SOD, MDA, GSH, and CAT of liver tissue and zonulin levels of colon tissue were detected by detection kit (Jiancheng Bioengineering, Nanjing, China). The serum LPS level was measured with detection kit (Jiancheng bioengineering, Nanjing, China) according to the manufacturer's instructions.

Real-time fluorescence quantitative PCR experiments. Total RNA was extracted from tissues using the RNA extraction kit (Fastagen, Shanghai, China) according to the manufacturer's instructions. Then, the total RNA concentration was detected by visible spectrophotometer and then reverse transcription was used to synthesize cDNA. Real-time PCR was carried out on an ABI 7500 real-time PCR system. The real-time quantitative PCR (qPCR) primers are shown in Table 1.

Morphological analysis. Tissue was collected and fixed in 4% paraformaldehyde. The sample was then dehydration embedded (in paraffin), sliced, and stained with hematoxylin and eosin (HE).

Fecal microbiota transplantation. The mice were randomly assigned into four groups (ATAB group, APAP group, ATAB.R group, and APAP.R group, $n = 6$ for each group). The ATAB.R and APAP.R groups received antibiotics intragastrically once daily for 5 days to deplete the gut microbiota. The feces of the donor mice (APAP group, ATAB group) were collected and resuspended in PBS at 0.125 g/mL. An amount of 0.15 mL was administered to the ATAB.R and APAP.R groups. After 3 days. Mice were intraperitoneally injected with 600 mg/kg APAP and were sacrificed at 24 h after APAP treatment.

Microbial analysis. Fresh fecal samples were collected using a metabolic cage and were stored at -80°C . The fecal contents were resuspended in PBS (pH 7.4) containing 0.5% Tween 20, and the fecal suspension was stirred with a stirrer to destroy the bacterial membrane. The samples were sequenced on the Illumina NovaSeq platform according to the manufacturer's recommendations. It mainly includes DNA extracted from fecal contents for amplification of variable region 4 (V4) of bacterial 16S rRNA gene by PCR. Then, the product was purified, and the library was prepared and sequenced. The *t* test, Wilcoxon rank sum test, and Tukey test were used for data processing to analyze the difference between alpha diversity index groups and beta diversity index groups. Other charts were implemented by R package.

Metabolomics analysis. The metabolites were extracted from feces, the supernatant collected, and the sample injected for LC-MS analysis. The chromatographic column was a Hypersil Gold column (100×2.1 mm, $1.9 \mu\text{m}$). The column temperature was 40°C , the flow rate was 0.2 mL/min, and the injection volume was $2 \mu\text{L}$. Mobile phase A, 0.1% formic acid; mobile phase B, methanol; gradient elutions, 0 to 1.5 min, 98% A and 2% B; 1.5 to 3 min, 98% A and 2% B; 3 to 10 min, 0% A and 100% B; 10 to 10.1 min, 98% A and 2% B; 10.1 to 13 min, 98% A and 2% B. Specific conditions of mass spectrometry, spray voltage, 3.5 kV; sheath gas flow rate, 35arb (a measure unit of gas flow rate); sheath gas flow rate, 35arb; aux gas flow rate, 10arb; capillary temperature, 320°C ; S-lens RF level, 60; aux gas heater temperature, 350°C .

Intestinal permeability. To determine intestinal mucosal barrier permeability, 20 h after APAP injection, mice were given FITC dextran 4 kDa (FD4, 500 mg/kg BW; Sigma) orally. After 4 h, blood samples were collected from the orbit, and serum was separated. The fluorescence intensity of glucose molecular protein in peripheral blood was measured by full wavelength automatic enzyme labeling instrument (Tecan spark) (excitation, 485 nm; emission, 525 nm). Paraffin sections of mice colon specimens were dewaxed and dehydrated. The fluorescence intensity of colon tissue was observed by fluorescence microscope (Olympus, Japan).

Application of SCFAs. The mice were randomly assigned into three groups (APAP group, SCFAs group, and control group; $n = 8$ for each group). For the SCFAs group, a short-chain fatty acid mixture (67.5 mM sodium acetate, 40 mM sodium propionate, 25.9 mM sodium butyrate) was dissolved in water and given to mice for free drinking for 7 days; then, APAP (600 mg/kg) was injected. For the APAP group and control group, the experimental method was the same as before. The blood and liver tissues of mice were collected after 24 h.

Statistical analysis. Data are expressed as means \pm standard error of the mean (SEM). An unpaired two-tailed Student's *t* test was used to assess differences between the two groups. Data sets involving more than two sets were evaluated using the Newman-Keuls test. The software MetaX was used to process the metabolomics data and for multivariate statistical analysis. Correlation analysis between different metabolites (Pearson correlation coefficient) was carried out in R (GraphPad Prism version 5.0; GraphPad Software). A *P* value of <0.05 was considered statistically significant.

Data availability. The 16S rRNA gene sequencing data are available at NCBI's Sequence Read Archive (SRA) database under BioProject accession number [PRJNA826304](https://www.ncbi.nlm.nih.gov/bioproject/PRJNA826304).

ACKNOWLEDGMENTS

This study was supported by NSFC81871242, National Key R&D Program of China (2018YFC1200603).

Z.Y. and Y.W. conceived and designed the experiments; X.S. and Q.C. performed the animal and molecular experiments; J.N., X.L., and T.Z. collected the samples; K.O., H.H., and J.Z. analyzed the data; Z.Y. wrote the paper.

We declare that we have no conflicts of interest.

REFERENCES

- Torres LB, Iruzubieta P, Ramos DF, Delgado TC, Taibo D, de Juan VG, Rey MV, Azkargorta M, Navasa N, Tussy PF, Franco IZ, Simon J, Otsoa FL, Ortega SL, Crespo J, Masson S, McCain MV, Villa E, Reeves H, Elortza F, Lucena MI, Alvarez MIH, Zorzano A, Andrade RJ, Lu SC, Mato JM, Anguita J, Rincón M, Chantar MLM. 2017. The mitochondrial negative regulator MCJ is a therapeutic target for acetaminophen-induced liver injury. *Nat Commun* 8:2068. <https://doi.org/10.1038/s41467-017-01970-x>.
- Sandhu N, Navarro V. 2020. Drug-induced liver injury in GI practice. *Hepatology* 4:631–645. <https://doi.org/10.1002/hep4.1503>.
- Andrade RJ, Aithal GP, Björnsson ES, Kaplowitz N, Kullak-Ublick GA, Larrey D, Karlsen TH. 2019. EASL clinical practice guidelines: drug-induced liver injury. *J Hepatol* 70:1222–1261. <https://doi.org/10.1016/j.jhep.2019.02.014>.
- Yan MZ, Huo YZ, Yin ST, Hu HB. 2018. Mechanisms of acetaminophen-induced liver injury and its implications for therapeutic interventions. *Redox Biol* 17:274–283. <https://doi.org/10.1016/j.redox.2018.04.019>.
- Du K, Ramachandran A, Jaeschke H. 2016. Oxidative stress during acetaminophen hepatotoxicity: sources, pathophysiological role and therapeutic potential. *Redox Biol* 10:148–156. <https://doi.org/10.1016/j.redox.2016.10.001>.
- Medzhitov R, Janeway C. 2000. Innate immune recognition: mechanisms and pathways. *Immunol Rev* 173:89–97. <https://doi.org/10.1034/j.1600-065x.2000.917309.x>.
- Kawai T, Akira S. 2011. Toll-like receptors and their crosstalk with other innate receptors in infection and immunity. *Immunity* 34:637–650. <https://doi.org/10.1016/j.immuni.2011.05.006>.
- Lee KY, Lee W, Jung SH, Park J, Sim H, Choi YJ, Park YJ, Chung Y, Lee BH. 2019. Hepatic upregulation of fetuin-A mediates acetaminophen-induced liver injury through activation of TLR4 in mice. *Biochem Pharmacol* 166:46–55. <https://doi.org/10.1016/j.bcp.2019.05.011>.
- Fisher JE, McKenzie TJ, Lillegard JB, Yu Y, Juskewitch JE, Nedredal GI, Brunn GJ, Yi ES, Malhi H, Smyrk TC, Nyberg SL. 2013. Role of Kupffer cells and Toll-like receptor 4 in acetaminophen-induced acute liver failure. *J Surg Res* 180:147–155. <https://doi.org/10.1016/j.jss.2012.11.051>.
- Shah N, de Oca MM, Cobos MJ, Tanamoto KI, Muroi M, Sugiyama KI, Davies NA, Mookerjee RP, Dhar DK, Jalan R. 2013. Role of Toll-like receptor 4 in mediating multiorgan dysfunction in mice with acetaminophen induced acute liver failure. *Liver Transpl* 19:751–761. <https://doi.org/10.1002/lt.23655>.
- Zhang C, Feng J, Du J, Zhuo ZY, Yang S, Zhang WH, Wang WH, Zhang SY, Iwakura Y, Meng GX, Fu YX, Hou BD, Tang H. 2018. Macrophage-derived IL-1 α promotes sterile inflammation in a mouse model of acetaminophen hepatotoxicity. *Cell Mol Immunol* 15:973–982. <https://doi.org/10.1038/cmi.2017.22>.

12. Chen SN, Tan Y, Xiao XC, Li Q, Wu Q, Peng YY, Ren J, Dong ML. 2021. Deletion of TLR4 attenuates lipopolysaccharide-induced acute liver injury by inhibiting inflammation and apoptosis. *Acta Pharmacol Sin* 42:1610–1619. <https://doi.org/10.1038/s41401-020-00597-x>.
13. Yoon E, Babar A, Choudhary M, Kutner M, Pysropoulos N. 2016. Acetaminophen-induced hepatotoxicity: a comprehensive update. *J Clin Transl Hepatol* 4:131–142. <https://doi.org/10.14218/JCTH.2015.00052>.
14. Krenkel O, Mossanen JC, Tacke F. 2014. Immune mechanisms in acetaminophen-induced acute liver failure. *Hepatobiliary Surg Nutr* 3:331–343. <https://doi.org/10.3978/j.issn.2304-3881.2014.11.01>.
15. Burgueño JF, Abreu MT. 2020. Epithelial Toll-like receptors and their role in gut homeostasis and disease. *Nat Rev Gastroenterol Hepatol* 17:263–278. <https://doi.org/10.1038/s41575-019-0261-4>.
16. Nahoum SR, Paglino J, Varzaneh FE, Edberg S, Medzhitov R. 2004. Recognition of commensal microflora by Toll-like receptors is required for intestinal homeostasis. *Cell* 118:229–241. <https://doi.org/10.1016/j.cell.2004.07.002>.
17. Neal MD, Sodhi CP, Jia H, Dyer M, Egan CE, Yazji I, Good M, Afrazi A, Marino R, Slagle D, Ma C, Branca MF, Prindle T, Grant Z, Ozolek J, Hackam DJ. 2012. Toll-like receptor 4 is expressed on intestinal stem cells and regulates their proliferation and apoptosis via the p53 up-regulated modulator of apoptosis. *J Biol Chem* 287:37296–37308. <https://doi.org/10.1074/jbc.M112.375881>.
18. Naito T, Mulet C, De Castro C, Molinaro A, Saffarian A, Nigro G, Bérard M, Clerc M, Pedersen AB, Sansonetti PJ, Pédrón T. 2017. Lipopolysaccharide from crypt-specific core microbiota modulates the colonic epithelial proliferation-to-differentiation balance. *mBio* 8:e01680-17. <https://doi.org/10.1128/mBio.01680-17>.
19. Dheer R, Santaolalla R, Davies JM, Lang JK, Phillips MC, Pastorini C, Pertejo MTV, Abreu MT. 2016. Intestinal epithelial Toll-like receptor 4 signaling affects epithelial function and colonic microbiota and promotes a risk for transmissible colitis. *Infect Immun* 84:798–810. <https://doi.org/10.1128/IAI.01374-15>.
20. Guo SH, Sadi RA, Said HM, Ma TY. 2013. Lipopolysaccharide causes an increase in intestinal tight junction permeability in vitro and in vivo by inducing enterocyte membrane expression and localization of TLR-4 and CD14. *Am J Pathol* 182:375–387. <https://doi.org/10.1016/j.ajpath.2012.10.014>.
21. Nighot M, Sadi RA, Guo SH, Rawat M, Nighot P, Watterson MD, Ma TY. 2017. Lipopolysaccharide-induced increase in intestinal epithelial tight permeability is mediated by Toll-like receptor 4/myeloid differentiation primary response 88 (MyD88) activation of myosin light chain kinase expression. *Am J Pathol* 187:2698–2710. <https://doi.org/10.1016/j.ajpath.2017.08.005>.
22. Schneider KM, Elfers C, Ghallab A, Schneider CV, Galvez EJC, Mohs A, Gui WF, Candels LS, Wirtz TH, Zuehlke S, Spittler M, Myllys M, Roulet A, Ouzerdine A, Lelouvier B, Kilic K, Liao LJ, Nier A, Latz E, Bergheim I, Thaiss CA, Hengstler JG, Strowig T, Trautwein C. 2021. Intestinal dysbiosis amplifies acetaminophen-induced acute liver injury. *Cell Mol Gastroenterol Hepatol* 11:909–933. <https://doi.org/10.1016/j.jcmgh.2020.11.002>.
23. Albillos A, de Gottardi A, Rescigno M. 2020. The gut-liver axis in liver disease: pathophysiological basis for therapy. *J Hepatol* 72:558–577. <https://doi.org/10.1016/j.jhep.2019.10.003>.
24. Schneider KM, Bieghs V, Heymann F, Hu W, Drey Mueller D, Liao LJ, Frissen M, Ludwig A, Gassler N, Pabst O, Latz E, Sellge G, Penders J, Tacke F, Trautwein C. 2015. CX3CR1 is a gatekeeper for intestinal barrier integrity in mice: limiting steatohepatitis by maintaining intestinal homeostasis. *Hepatology* 62:1405–1416. <https://doi.org/10.1002/hep.27982>.
25. Yan AW, Fouts DE, Brandl J, Stärkel P, Torralba M, Schott E, Tsukamoto H, Nelson KE, Brenner DA, Schnabl B. 2011. Enteric dysbiosis associated with a mouse model of alcoholic liver disease. *Hepatology* 53:96–105. <https://doi.org/10.1002/hep.24018>.
26. Seki E, Schnabl B. 2012. Role of innate immunity and the microbiota in liver fibrosis: crosstalk between the liver and gut. *J Physiol* 590:447–458. <https://doi.org/10.1113/jphysiol.2011.219691>.
27. Chopky DM, Grakoui A. 2020. Contribution of the intestinal microbiome and gut barrier to hepatic disorders. *Gastroenterology* 159:849–863. <https://doi.org/10.1053/j.gastro.2020.04.077>.
28. Fouts DE, Torralba M, Nelson KE, Brenner DA, Schnabl B. 2012. Bacterial translocation and changes in the intestinal microbiome in mouse models of liver disease. *J Hepatol* 56:1283–1292. <https://doi.org/10.1016/j.jhep.2012.01.019>.
29. Wang YW, Gong DD, Yao CX, Zheng F, Zhou TT, Cao QX, Zhu XH, Wang MR, Zhu J. 2020. Human monoclonal anti-TLR4 antibody negatively regulates lipopolysaccharide-induced inflammatory responses in mouse macrophages. *Mol Med Rep* 22:4125–4134. <https://doi.org/10.3892/mmr.2020.11500>.
30. Ding L, Gong YH, Yang ZF, Zou BJ, Liu XL, Zhang BM, Li J. 2019. Lactobacillus rhamnosus GG ameliorates liver injury and hypoxic hepatitis in rat model of CLP-induced sepsis. *Dig Dis Sci* 64:2867–2877. <https://doi.org/10.1007/s10620-019-05628-0>.
31. Fang TJ, Guo JT, Lin MK, Lee MS, Chen YL, Lin WH. 2019. Protective effects of Lactobacillus plantarum against chronic alcohol-induced liver injury in the murine model. *Appl Microbiol Biotechnol* 103:8597–8608. <https://doi.org/10.1007/s00253-019-10122-8>.
32. Lv LX, Yao CY, Yan R, Jiang HY, Wang QQ, Wang KC, Ren SQ, Jiang SD, Xia JF, Li SJ, Yu Y. 2021. Lactobacillus acidophilus LA14 alleviates liver injury. *mSystems* 6:e00384-21. <https://doi.org/10.1128/mSystems.00384-21>.
33. Raftar SKA, Ashrafi F, Yadegar A, Lari A, Moradi HR, Shahriari A, Azimirad M, Alavifard H, Mohsenifar Z, Davari M, Vaziri F, Moshiri A, Siadat SD, Zali MR. 2021. The protective effects of live and pasteurized Akkermansia muciniphila and its extracellular vesicles against HFD/CCl4-induced liver injury. *Microbiol Spectr* 9:e00484-21. <https://doi.org/10.1128/Spectrum.00484-21>.
34. Seo B, Jeon K, Moon S, Lee K, Kim WK, Jeong H, Cha KH, Lim MY, Kang W, Kweon MN, Sung J, Kim W, Park JH, Ko GP. 2020. Roseburia spp. abundance associates with alcohol consumption in humans and its administration ameliorates alcoholic fatty liver in mice. *Cell Host Microbe* 27:25–40. <https://doi.org/10.1016/j.chom.2019.11.001>.
35. Scott KP, Martin JC, Campbell G, Mayer CD, Flint HJ. 2006. Whole-genome transcription profiling reveals genes up-regulated by growth on fucose in the human gut bacterium “Roseburia inulinivorans”. *J Bacteriol* 188:4340–4349. <https://doi.org/10.1128/JB.00137-06>.
36. Louis P, Hold GL, Flint HJ. 2014. The gut microbiota, bacterial metabolites and colorectal cancer. *Nat Rev Microbiol* 12:661–672. <https://doi.org/10.1038/nrmicro3344>.
37. Koh A, De Vadder F, Datchary PK, Bäckhed F. 2016. From dietary fiber to host physiology: short-chain fatty acids as key bacterial metabolites. *Cell* 165:1332–1345. <https://doi.org/10.1016/j.cell.2016.05.041>.
38. Chaudhari SN, McCurry MD, Devlin AS. 2021. Chains of evidence from correlations to causal molecules in microbiome-linked diseases. *Nat Chem Biol* 17:1046–1056. <https://doi.org/10.1038/s41589-021-00861-z>.
39. Krautkramer KA, Fan J, Bäckhed F. 2021. Gut microbial metabolites as multi-kingdom intermediates. *Nat Rev Microbiol* 19:77–94. <https://doi.org/10.1038/s41579-020-0438-4>.
40. Han H, Jiang Y, Wang MY, Melaku M, Liu L, Zhao Y, Everaert N, Yi B, Zhang HF. 2021. Intestinal dysbiosis in nonalcoholic fatty liver disease (NAFLD): focusing on the gut–liver axis. *Crit Rev Food Sci Nutr* 18:1–18. <https://doi.org/10.1080/10408398.2021.1966738>.
41. Macfarlane GT, Macfarlane S. 2012. Bacteria, colonic fermentation, and gastrointestinal health. *J AOAC Int* 95:50–60. https://doi.org/10.5740/jaoacint.sge_macfarlane.
42. Camilleri M, Vella A. 2022. What to do about the leaky gut. *Gut* 71:424–435. <https://doi.org/10.1136/gutjnl-2021-325428>.
43. Yang RK, Zou XP, Tenhunen J, Zhu ST, Kajander H, Koskinen ML, Tonnessen TI. 2014. HMGb1 neutralization is associated with bacterial translocation during acetaminophen hepatotoxicity. *BMC Gastroenterol* 14:66. <https://doi.org/10.1186/1471-230X-14-66>.
44. Wu CT, Deng JS, Huang WC, Shieh PC, Chung MI, Huang GJ. 2019. Salvia-nolic acid C against acetaminophen-induced acute liver injury by attenuating inflammation, oxidative stress, and apoptosis through inhibition of the Keap1/Nrf2/HO-1 signaling. *Oxidative Med Cell Longevity* 2019:9056845.